Supporting Information

Wu et al. 10.1073/pnas.0811785106

SI Methods

Tissues and Cells. The normal breast tissues were obtained from discarded material from patients undergoing elective reduction mammoplasty. The ages of the donors used in this study were 52 years for donor 1, 34 years for donor 2, 61 years for donor 3, 47 years for donor 4, and 55 years for donor 5. The patients were not from a high-risk cohort. Immortalized human breast fibroblasts, RMF and RMF-HGF, primary human breast fibroblasts, and organoids were isolated and generated from reduction mammoplasty tissue as described previously (1).

Clearing and Humanizing Mouse Fat Pads. Immunocompromised NOD/SCID mice (Jackson Laboratory) were purchased and maintained in-house under aseptic sterile conditions. All of the animal procedures have been approved by the AVEO Institutional Animal Care and Use committee. Endogenous mouse mammary epithelium was cleared form the fourth inguinal mammary gland and humanized through injection with immortalized human breast fibroblasts (RMF or RMF-HGF) (1). One day before injection, half of the fibroblasts were treated with 2 milliunits/mL bleomycin for 30 min. On the day of injection, a 1:1 mix of bleomycin-treated fibroblasts and untreated fibroblasts was injected into the cleared fat pads at 0.5×10^6 cells per injection site. Two weeks following humanization, epithelial cells were introduced in the glands.

Infection and Injection of Human Breast Organoids. The medium for culturing organoids during infection was composed of 10 ng/mL human insulin, 10 μg/mL human EGF, and 10 μg/mL hydrocortisone. Briefly, about 50 μL of organoid pellet was resuspended in 1 mL of human mammary epithelial medium (HMEM) (1) containing 10^5 to10^7 cfu lentiviruses expressing the gene of interest. The organoid/virus mixture was subjected to 1 round of infection by spinning for 90 min at $405 \times g$. Subsequent rounds of spin infection were performed between approximately 2 and 20 h after the previous infection. Within 4–18 h after the last infection, the infected organoids were injected into humanized fat pads without selection. A total of 30–50 organoids were injected into a humanized fat pad in the presence of 0.25×10^6 bleomycin-treated RMF-HGFs and 0.25×10^6 nontreated RMF-HGFs. The cell preparations were resuspended in a 1:1 mix of collagen–matrigel mix and injected in a volume of about 30–50 μL per injection site.

Constructs and Virus Production. The *p53* shRNA sequence was as described in Brummelkamp et al. (2). A 2.7-kb *SV40er* DNA fragment was subcloned from the pSV3-dhfr vector (ATCC no. 37147). We obtained the $KRAS^{G12V}$ cDNA construct as a gift from Lynda Chin (Harvard University Medical School, Boston, MA). The *HER2* cDNA used in making this construct was $HER2^{V659E}$. The accession number for wild-type *HER2* cDNA is M11730. Site-directed mutagenesis was used to change amino acid residue 659 from V to E. The cDNA clone for the catalytic subunit of *PI3K*, *PIK3CA*, was purchased from Open Biosystems (catalogue no. EHS1001-1259687). Site-directed mutagenesis was used to change amino acid residue 1047 from H to R. A cyclin D1 (*CCND1*) cDNA clone was ordered from American Type Culture Collection (catalog no. MGC-2316). A wild-type human *p53* cDNA clone was purchased from American Type Culture Collection (catalogue no. MGC-646). Site-directed mutagenesis was used to change amino acid residue 175 from R to H.

Virus constructs used in generating *p53sh/KRAS/GFP* and *p53sh/HER2* recombined glands were pLenti-U6-*p53*shRNA-CMV-$KRAS^{G12V}$+SV40-*GFP* and pLenti-U6-*p53*shRNA-CMV-$HER2^{V659E}$, separately. Constructs used in generating *KRAS/SV40er* tumors were pLenti-CMV-*SV40er* and pLenti-CMV-$KRAS^{G12V}$+SV40-*GFP*. Constructs used in generating *HER2/SV40er* tumors were pLenti-CMV-*SV40er* and pLenti-CMV-$HER2^{V659E}$. Constructs used in generating *KRAS/PIK3CA/p53R175H/CCND1* tumors were pLenti-CMV-$KRAS^{G12V}$+SV40-*GFP*, pLenti-CMV-*PIK3CA-myr*+CMV-*CCND1*, and pLenti-CMV-*p53R175H*.

Genotyping PCR and RT-PCR Analysis of KRAS/p53R175H/CCND1/PIK3CA Tumors. Genomic DNA was extracted from the *KRAS/p53R175H/CCND1/PIK3CA* tumors and used in standard PCR to confirm lentiviral construct integration into the tumor cell genome. The primer pairs used in PCR were designed to amplify gene-specific cDNA fragments, which should be present in the virus-integrated tumor cell genome but not in the genomic DNA of normal human samples. Primer sequences are as follows: PIK3CA (167 bp): F-GATTGACAGACAACCATAAGG/R-GATTGACAGACAACCATAAGG; CCND1 (158 bp): F-GATGCCAACCTCCTCAACGA/R-TGTTCCTCGCAGACCTCCAG; p53R175 (121 bp): F-AACCTACCAGGGCAGCTACG/R-GCAGGTCTTGGCCAGTTGGC; KRAS (137 bp): F-GTAGGCAAGAGTGCCTTGAC/R-GCTGTGTCGAGAATATCCAAG; and β-actin (200 bp): F-TTCCTGGGCATGGAGTCCTG/R-AGGAGCAATGATCTTGATCTTC.

RNA was extracted from the *KRAS/p53R175H/CCND1/PIK3CA* tumors and used in standard RT-PCR to confirm expression of lentiviral construct-specific transcripts. The primer pairs were designed such that one primer was from the lentiviral vector, and the other one was from the gene to be analyzed. In this way, only transcripts from the lentiviral contructs, but not normal human genomic locus, could be amplified. Primer sequences are as follows: PIK3CA (242 bp): F- GAATGATGCACATCATGGTGG/R-TCCAGTCGGGCAAATTATATAG; CCND1 (27 6bp): F-CCTGCTGGAGTCAAGCCTGC/R-CAACCACTTTGTACAAGAAAGC; p53R175H (225 bp): F-TGACCTCCATAGAAGACACC/R-CTGACTGCGGCTCCTCCATG; KRAS (149 bp):F-TAGAGGATCCACTAGTACCACCATG/R-GCTTCCTGTAGGAATCCTCTATTG; and β-actin (200 bp): F-TTCCTGGGCATGGAGTCCTG/R-AGGAGCAATGATCTTGATCTTC.

Monitoring Tumor Development. *HER2/SV40er* human breast tissue recombinants were collected at the following time points after implantation: 7 days, 10 days, 17 days, 25 days, 35 days, and 45 days. Six tissue recombinants were collected at each time point and subjected to histopathological analysis. The human breast outgrowths were classified according to the following criteria: (*i*) Epithelial structures less than 5 viable cell layers thick and without marked, uniform nuclear atypia were classified as hyperplastic; (*ii*) Structures more than 5 layers thick with a relatively simple outline (usually circular) and most cells showing nuclear atypia were classified as DCIS; (*iii*) Structures with uniform nuclear atypia, more than 5 layers thick (generally), and a complex (infiltrative-appearing) outline were classified as invasive.

Tumor Treatment. Mice bearing *HER2/SV40er* tissue recombinants were treated for 4 days between days 26 and 29 after

implantation. The treatment groups are as follows (6 tissue recombinants per group): vehicle, 100-mpk AV412, and 20-mpk trastuzumab. AV412 was dosed daily for 4 consecutive days. Trastuzumab was dosed one time each on days 26 and 29. The treated tissue recombinants were harvested at days 1 and 3 following the last dosing (days 30 and 32 after implantation, separately). The percent of apoptotic/necrotic area in the tissue recombinants was quantified by measuring active caspase-3-positive areas in each tumor outgrowth by using the National Institutes of Health ImageJ program (http://rsb.info.nih.gov/ij/).

1. Kuperwasser C, et al. (2004) Reconstruction of functionally normal and malignant human breast tissues in mice. *Proc Natl Acad Sci USA* 101:4966–4971.
2. Brummelkamp TR, Bernards R, Agami R (2002) A system for stable expression of short interfering RNAs in mammalian cells. *Science* 296:550–553.

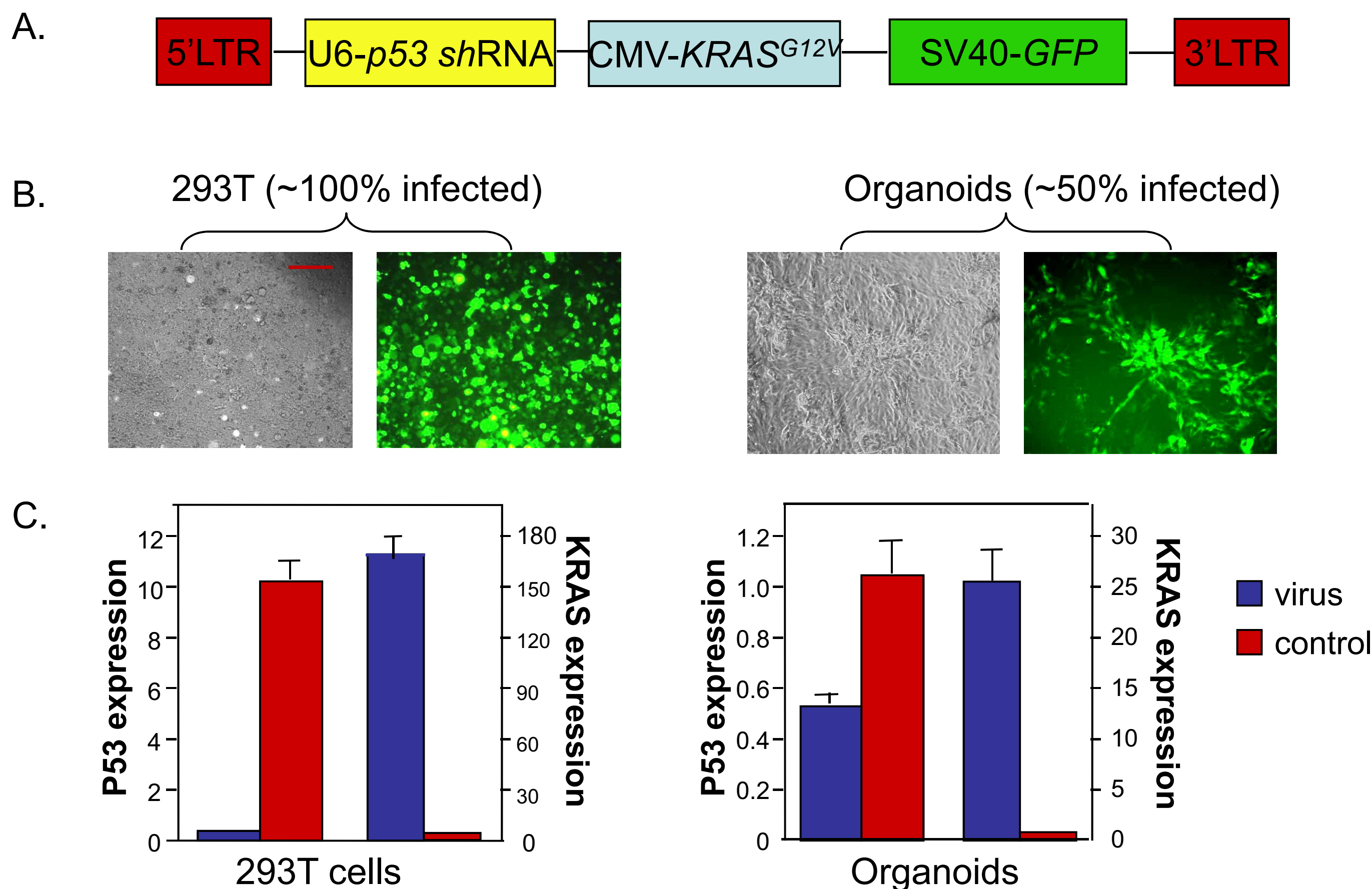

Fig. S1. Primary human breast epithelial cells can be infected through lentiviral transduction of nondividing organoids, establishing an efficient gene delivery method for both shRNAs and oncogenes in human cells. (*A*) Schematic representation of lentiviral vector, *p53sh/KRAS/GFP*. This is a self-inactivating lentiviral expression vector capable of driving expression of an shRNA hairpin loop with the U6 promoter, an oncogene with the CMV promoter, and the GFP with the SV40 promoter. Lentiviruses were generated for this vector and used to infect 293T cells and primary human breast epithelial organoids. (*B*) Bright-light and GFP micrographs of infected 293T cells or epithelial organoids following lentiviral infection. Examination of GFP-positive cells revealed that 100% of 293T cells and nearly 50% of epithelial cells were infected with the *p53sh/KRAS/GFP* lentiviruses. (Scale bar: 0.1 μm. The magnification is the same for all 4 images.) (*C*) Quantitative RT-PCR analysis of *p53* and *KRAS* expression levels in the infected 293T cells and organoids. Compared with mock infected cells (control), ≈97% knockdown of *p53* transcription was achieved in 293T cells, and when normalized to infection efficiency, nearly 100% knockdown of *p53* transcription was achieved in epithelial organoids through infection with these lentiviruses. In addition, nearly 100% knockdown of *p53* transcription was achieved in both 293T cells and in epithelial organoids (given that only 50% of organoids were infected) through lentiviral system.

Fig. S2. An electronic copy of Fig. 1 for detailed view of the histopathology of HIM tissue recombinants. (*A*) Premalignant lesions and CIS developed in vivo from human breast tissue recombinants overexpressing *HER2 or KRAS* with concomitant knocking down of *p53*. (*Ai*) GFP whole mount of a reconstituted *p53sh/KRAS/GFP* human breast tissue reveals KRAS-lentivirus expression in both normal TDLU structures (*Inset*) as well as in hyperplasic nodule (HYP). (Scale bar: 0.5 mm.) (*Aii*) H&E of the *p53sh/KRAS/GFP* hyperplastic outgrowth in *Ai*. (*Aiii*). IHC-stained serial section of *Aii* demonstrating the filling of the luminal space with epithelial cells. (*Aiv–Aix*). Histological analysis of *p53sh/HER2* tissue recombinants revealed both hyperplastic (*iv–vi*) and CIS outgrowth (*Avii–Aix*) from transduced organoids (*Aiv* and *Avii*). (Scale bars: *Ai*, 0.5 mm; *Aii–Aix*, 50 μm.) (*B*) Poorly differentiated, invasive human carcinomas developed in vivo from *HER2/SV40er* and *KRAS/SV40er* human breast tissue recombinants. Histological analysis of *HER2/SV40er* (*Bi–Bv*) and *KRAS/SV40er* (*Bvi–Bx*) tumors. H&E-stained sections (*Bi* and *Bvi*) and IHC analysis on serial sections with αSMA (*Bii* and *Bvii*), pan-cytokeratin (Pan-CK; *Biii* and *Bviii*), SV40 LT (*Biv* and *Bix*), and *HER2* (*Bv*) demonstrated that tumors were derived from epithelial cells that overexpressed the transduced oncogenes. RNA in situ analysis (*Bx*) confirmed the expression of *KRAS* in *KRAS/SV40er* tumors. (Scale bar: 100 μm.) (*C*) Invasive ductal adenocarcinoma developed in vivo from *KRAS/p53R175H/CCND1/PIK3CA* tissue recombinants. H&E-stained sections of genetically engineered HIM tumor (*Ci* and *Cii*) revealed that both samples are invasive ductal adenocarcinoma with prominent glandular architecture and low mitotic index. IHC-stained serial sections of HIM tumors with pan-cytokeratin (Pan-CK; *Cii* and *Cvi*), p53 (*Ciii* and *Cvii*), and αSMA (*Civ* and *Cviii*) revealed mutant p53-positive epithelial cancer cells surrounded by myofibroblastic stroma. (Scale bar: 50 μm.)

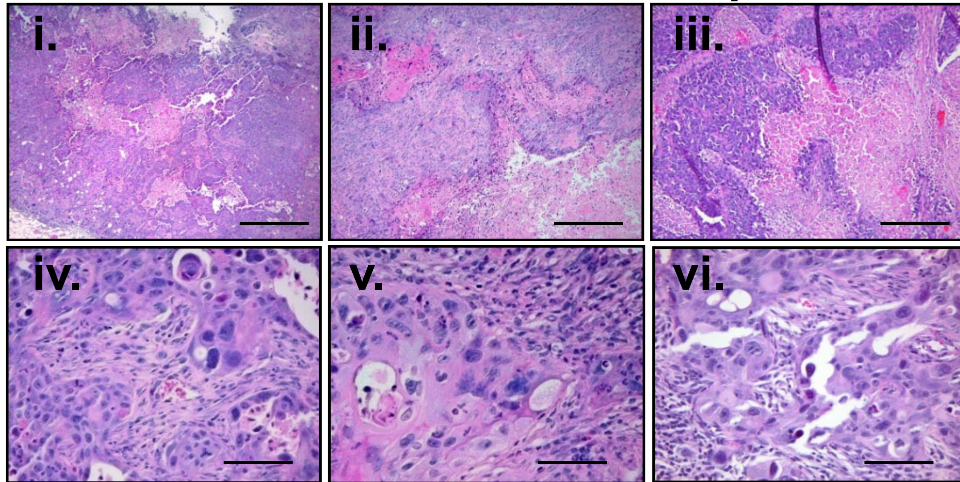

Fig. S3. Comparative histology of genetically engineered HIM breast tumors (*i*, *ii*, *iv*, and *v*) and patient-derived breast cancer tissue (*iii* and *vi*). H&E-stained sections revealed that both the HIM tumors and the patient breast cancer are highly malignant human carcinomas. The invasive growth pattern by nests and islands of tumor cells and the considerable cellular pleomorphism in the *HER2/SV40er* and *KRAS/SV40er* tumors are characteristic of some highly malignant human tumors. In addition, the tumors contained prominent areas of stromal desmoplasia, a feature present in many human breast carcinomas. (Scale bar: *i*–*iii*, 200 μm; *iv*–*vi*, 50 μm.)

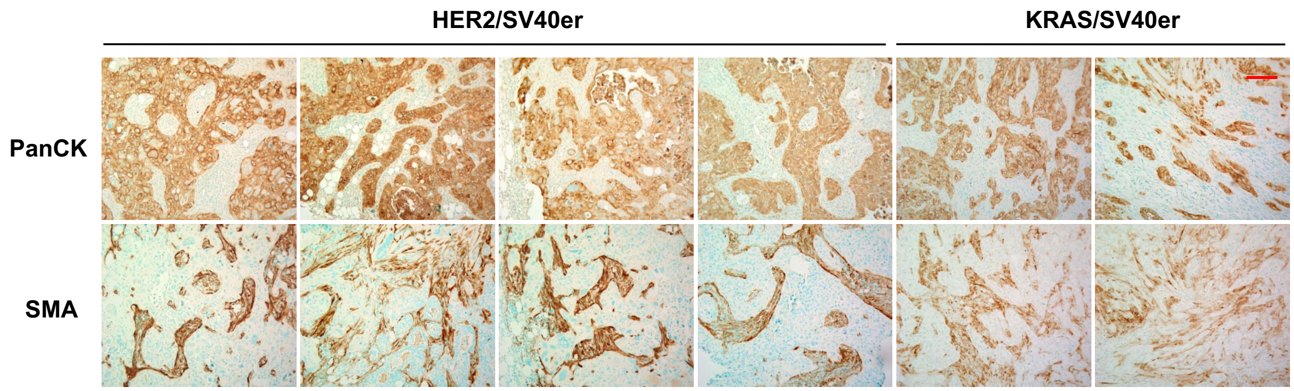

Fig. S4. Additional images to illustrate stromal desmoplasia in *HER2/SV40er* and *KRAS/SV40er* tumors, which was evidenced by positive α*SMA* staining on the tumor sections. (Scale bar: 100 μm.)

Fig. S5. Established HIM models resemble basal and/or basal-HER2 subtypes of human breast cancer. Both the KRAS/SV40er and the *KRAS/p53R175H/CCND1/PIK3CA* tumors are ER$^-$/PR$^-$/CK5/6$^+$/p63$^+$/HER2$^-$, whereas the HER2/SV40er tumors are ER$^-$/PR$^-$/CK5/6$^+$/p63$^+$/HER2$^+$. *Inset a* is a control ER staining on a cross-section from a human ER$^+$/PR$^+$ breast cancer specimen. *Inset b* is a control PR staining on a cross-section from a human ER$^+$/PR$^+$ breast cancer specimen. The *Insets* have the same magnification as the other images in ER and PR. (Scale bar: 50 μm.)

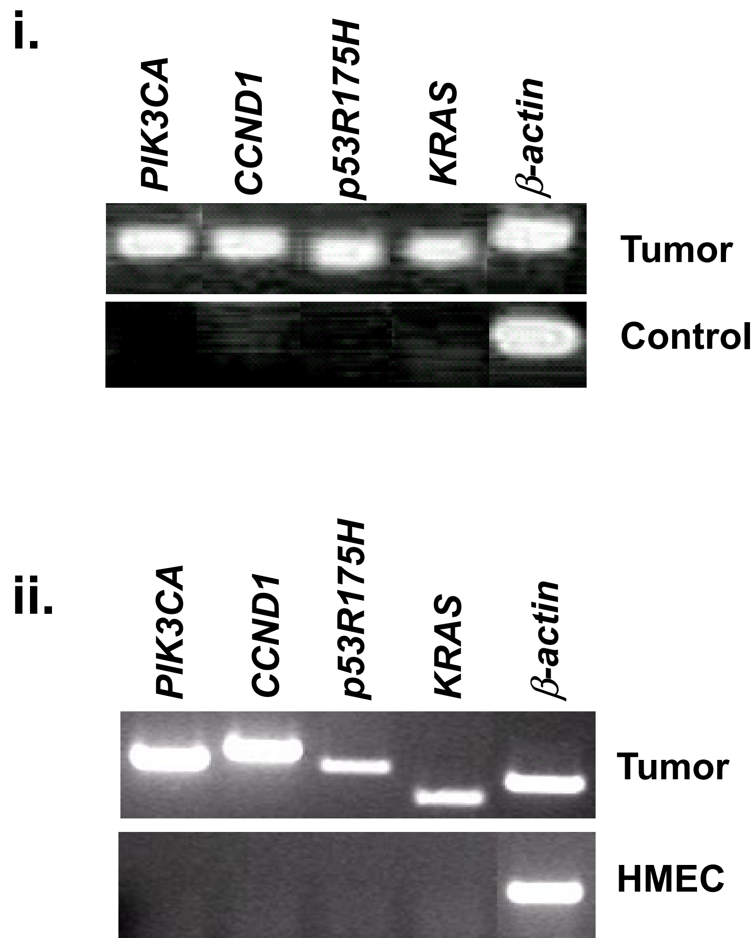

Fig. S6. Invasive ductal adenocarcinoma developed in vivo from *KRAS/p53R175H/CCND1/PIK3CA* tissue recombinants. (*i*) Stable integration of viral DNA into human cancer cells was detected by PCR analysis. Genomic DNA was extracted from tumor tissue and subjected to PCR with primer pairs specific for genomic fragment introduced by lentiviruses. Genomic DNA from normal human sample was used as control template. Primer pair specific for human β-actin was used as control primer. (*ii*) Expression of genetic elements introduced through lentiviruses. RNA was extracted from tumor tissue and subjected to RT-PCR with primer pairs specific for the transcripts introduced by lentiviruses. RNA from primary HMECs was used as control template.

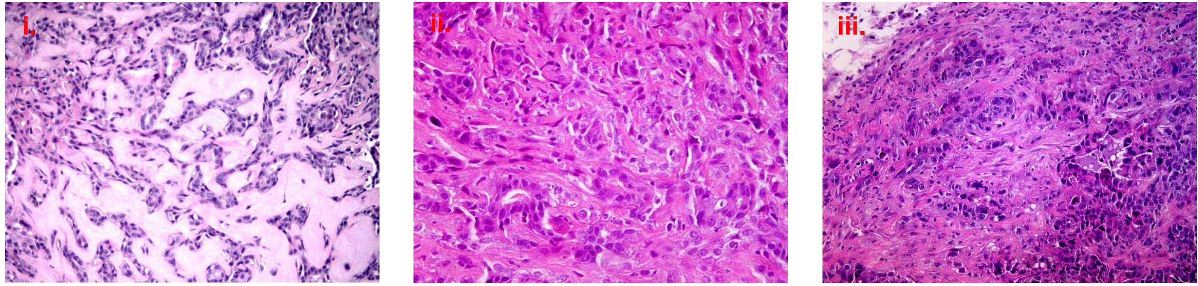

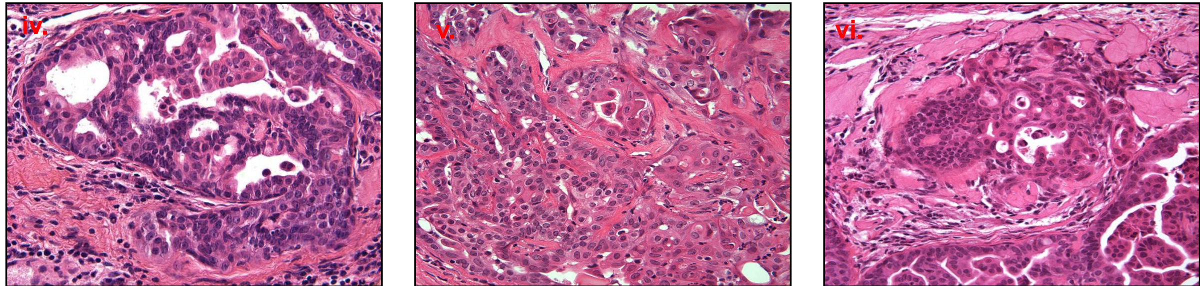

Fig. S7. Characterization of *KRAS/p53R175H/CCND1/PIK3CA* tissue recombinants reconstituted with organoids derived from 2 different patients: patient no. 1 (*i–iii*) and patient no. 2 (*iv–vi*). In this set of experiments, the *KRAS/p53R175H/CCND1/PIK3CA* tissue recombinants from patient no. 1 gave rise to well-to-moderately differentiated adenocarcinoma, whereas the *KRAS/p53R175H/CCND1/PIK3CA* tissue recombinants from patient no. 2 gave rise to various preneoplastic and malignant lesions, including DCIS and hyperplasia, as well as emergence of invasive carcinoma. Glands contained tumor growth patterns that resembled that of the cribriform subtype of human DCIS (*iv*), whereas other outgrowths predominantly appeared to be hyperplasia with focal areas of emerging invasive carcinoma (*v* and *vi*). Despite the greater variability of precursor lesions, emerging invasive carcinoma was observed in 95% (19 of 20) of the glands.

Table S1. Summary on the histopathologic analysis of *p53 sh/HER2* and *p53 sh/KRAS/GFP* tissue recombinants

Genotype	Collection period, month	No. of tissue recombinants	Frequency of hyperplasia, % (no.)	Frequency of CIS, % (no.)
p53 sh/HER2	1–5	10	100 (10 of 10)	0 (0 of 10)
	6–10	14	100 (14 of 14)	21.5 (3 of 14)
	1–10 (combined)	24	100 (24 of 24)	12.5 (3 of 24)
p53 sh/KRAS/GFP	1–5	4	100 (4 of 4)	0 (0 of 4)
	6–10	12	100 (12 of 12)	0 (0 of 12)
	1–10 (combined)	16	100 (16 of 16)	0 (0 of 16)

Table S2. Summary on the kinetics of tumor propagation

Oncogene	Tumor line	No. of sites injected	No. of tumors collected	% of tumor take	Latency, weeks
HER2/SV40er	H1	10	10	100	6
	H2	6	6	100	5
	H3	7	7	100	8
	H4	6	6	100	7
	H5	7	7	100	9
	H6	6	6	100	6
KRAS/SV40er	K1	10	5	50	9
	K2	6	6	100	6
	K3	5	2	40	9
	K4	4	2	50	12 and 26
	K5	4	4	100	8
	K6	6	5	83	6

Table S3. Summary on tumor frequency from various tissue recombination derived from organoids from donor 1 and donor 2

Genetic combination	Organoids	Tumor frequency	Tumor latency, month
p53 sh/HER2	Donor 1	0 of 17	N/A
	Donor 2	0 of 16	N/A
p53 sh/KRAS/GFP	Donor 1	0 of 17	N/A
	Donor 2	0 of 16	N/A
HER2/SV40er	Donor 1	14 of 14	1.5–3.5
	Donor 2	6 of 6	1.5–2
KRAS/SV40er	Donor 1	10 of 10	1.5 - 3.5
	Donor 2	N/A	N/A
KRAS/p53R175H/CCND1/PIK3CA	Donor 1	18 of 20	2–9
	Donor 2	19 of 20	2–7